Thesis Proposal

Fletcher Young

Case Western Reserve University
Cleveland, OH 44106
fry2@case.edu

This document is meant to serve as documentation of research completed thus far.

1 Introduction and Significance

2 Background

3 Research Strategy

3.1 Aim 1 - Develop a physiologically relevant hindlimb model of the rat musculature

To accomplish this aim, a three dimensional model was created in Animatlab with attachment points and muscle parameters based on data in the literature. The development of this model includes both the biomechanical setup in Animatlab and the code basis to analyze its motion. This model lacks the neural control aspect critical to the project but serves as a platform for biomechanical analysis and development. The development of this model is developed from fundamental principles with each component expanding on the previous development.

This model serves as a development of the work completed by Dr. Alex Hunt in completion of his PhD thesis[1][2][3]. In Dr. Hunt's model, a rat model demonstrated locomotory capabilities through neural control of hindlimb muscles. This work developed the process for decomposing biomechanical movements into the motorneuron signals necessary to generate them. However, this work had the benefit of not having to consider the impact of biarticular muscles, a complication which negates the use of a simple one-to-one CPG to musculature system. In the development of a more biologically relevant model, the inclusion of the full hindlimb musculature must be considered.

As a first step in developing a full-muscle hindlimb model, the attachment point of every hindlimb muscle was considered. Initially, this work implemented the attachment points derived by Dr. Will Johnson[4] in which he uses 3D mapping to develop xyz-coordinates for muscle attachment points. The implementation of Johnson's attachment points were presented as part of a project presentation at Living Machines 2018[5]. Johnson's work was useful from an engineering design standpoint but was unusable for two reasons: the coordinates required hand-tuned scaling in order to map correctly onto the existing bone structures and including only the insertion and origins did not accommodate muscle wrapping via points. For this reason, a more nuanced approach was implemented for the muscle attachment points.

Muscle paths were defined based on the descriptions by Greene's 1955 publication Anatomy of the Rat[6], a primer containing diagrams and descriptions of every system in the rat. Based on this information and the identification of bony landmarks in the 3D bone scans, muscle paths were implemented. Animatlab's muscle objects are not collision-based, meaning they can pass directly through bones. For muscles that pass closely over bones (such as knee extensors like the vastii muscles), muscle paths include via points. These via points are stationary relative to the bone coordinate frames.

Once muscle paths were defined for every muscle, muscle parameters were developed. Animatlab uses a linear Hill muscle, shown in Figure 1, model which abides by the equation:

$$\frac{dT}{dt} = \frac{k_{SE}}{c}\left[k_{PE}(L - L_{rest}) + c\dot{L} - \left(1 + \frac{k_{PE}}{k_{SE}}\right)T + A_m A_l\right]$$

$$0 = \frac{k_{SE}}{c}\left[k_{PE}(L - L_{rest}) - \left(1 + \frac{k_{PE}}{k_{SE}}\right)T^* + A_m A_l\right]$$

$$T^*(L) = \left(\frac{1}{1 + \frac{k_{PE}}{k_{SE}}}\right)\left[k_{PE}(L - L_{rest}) + A_m^*\left(1 - \frac{(L - L_{rest})^2}{.25L_{rest}^2}\right)\right]$$

$$T^*(L_{rest}) = F_o = \frac{A_m^*}{1 + \frac{k_{PE}}{k_{SE}}}$$

$$T^*(1.4L_{rest}) = .5F_o = \frac{.4L_{rest}k_{PE} + .36A_m^*}{1 + \frac{k_{PE}}{k_{SE}}}$$

$$T^*(1.5L_{rest}) = .01F_o = \frac{.5L_{rest}k_{PE}}{1 + \frac{k_{PE}}{k_{SE}}}$$

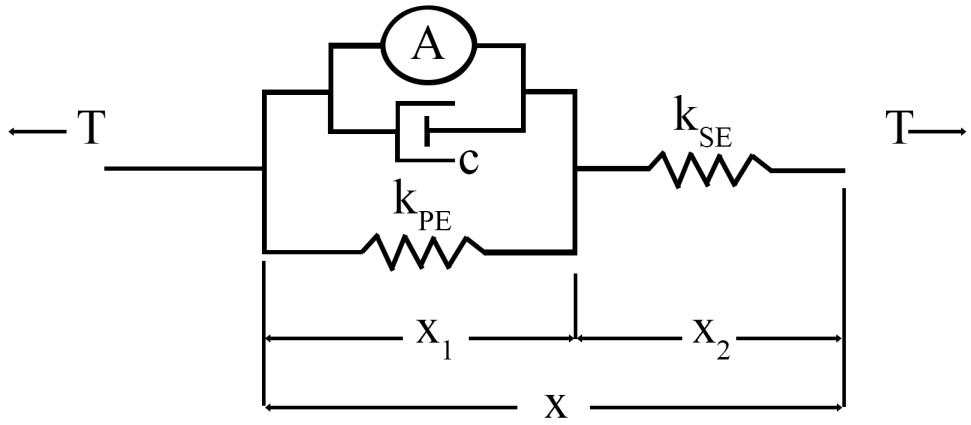

Fig. 1: The Linear Hill Muscle Model

Where T is the muscle tension, k_{SE} is the serial element stiffness, k_{PE} is the parallel element stiffness, c is the muscle damping, A is the active muscle unit, L is the length of the muscle, L_{rest} is the length of muscle at which tension is zero. This model demands explicit statements for these different variables, a data set that has not been found in the literature. By using muscle parameters examined by Johnson[7] and Eng[8], it is possible to develop these muscle parameters. Using the guidance of Zajac[9], these muscle parameters were related to Hill parameters. Individual parameters are discussed individually as follows.

Serial Element Stiffness The series elastic element (Kse) represents the tendon stiffness of the muscle. By using the tendon slack length (TSL) for each muscle[7], the serial element stiffness was calculated from a generic stress-strain curve[9], shown in Figure 2. Normalized tendon stress equals normalized tendon force under the assumption that the optimal tendon stress is 32MPa.

Under the assumption that within the range of $[1, 3.5]F_{max}$, nominal tendon strain is [3.3,10]%:

$$\epsilon^T = \frac{\Delta L^T}{L_s^T} = \frac{L^T - L_s^T}{L_s^T} = \frac{L^T}{L_s^T} - 1$$

$$K_{se} = \frac{\Delta F}{\Delta L} = \frac{\Delta F}{(\Delta\epsilon + 1)L_s^T} = \frac{3.5F_o^M - F_o^M}{1.1L_s^T - 1.033L_s^T} = 37.5\frac{F_o^M}{L_s^T}$$

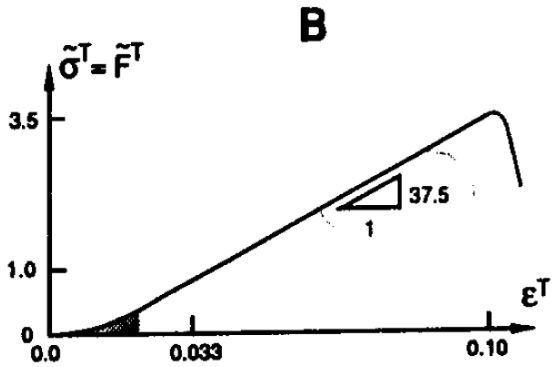

Fig. 2: Zajac's normalized stress-strain curve.

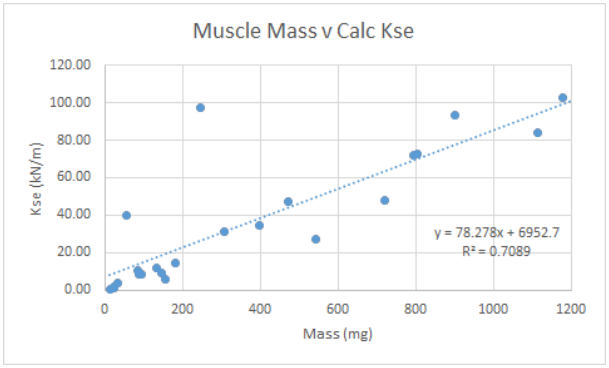

Fig. 3: Zajac2

where ϵ^T is the normalized tendon strain, L^T is the tendon length, and L_s^T is the TSL. While this calculation is convenient for muscles with defined TSL, many muscles lack a reliable TSL measurement. For these muscles, a trendline was established between muscle mass and k_{SE}.

Parallel Element Stiffness The parallel elastic element can be calculated if we assume that the series and parallel elastic elements absorb all tension when the muscle is at a set length. By this assumption, we can treat the muscle as a simple two-spring system under load. Assuming the muscle exerts 70% of their maximum force when fully contracted and knowing the values of K_{se}, we can find K_{pe}.

$$\begin{aligned} F &= K_{eq}x \\ \Delta F &= K_{eq}\Delta L \\ (F_{max} - .7F_{max}) &= K_{eq}(L_{max} - L_{min}) \\ .3F_{max} &= \frac{K_{se}K_{pe}}{K_{se} + K_{pe}}(L_{max} - L_{min}) \\ K_{pe} &= \frac{.3F_{max}K_{se}}{K_{se}(L_{max} - L_{min}) - .3F_{max}} \end{aligned}$$

where F_{max} is the maximum muscle force[7], K_{se} is the series element stiffness, and the length limits determined by computing the muscle length profiles.

Damping

$$\begin{aligned} c &= \frac{F_{max}}{v_f^M * \left(\frac{L_f}{L_m}\right)} \\ c &= \frac{F_{max}}{v_{max}} \end{aligned}$$

Muscle Tension Curves

Length-Tension Curve The length-tension (LT) curve of muscle is used to map the length of the muscle to to its force-generating capabilities. A general form of a muscle's LT curve[9] is shown in Fig. 4. At an optimal resting length, a muscle is capable of producing an optimal isometric force. Above or below this optimal length, the muscle's ability to produce force is diminished. As the muscle is pulled to a supraoptimal length, passive forces within the muscle begin to accumulate, enhancing the muscle's ability to generate tension simply due to its structure. Animatlab presents a simplified version of the LT curve, shown in Fig. 4. The muscle width is a property that Animatlab uses to define its simplified length-tension curve.

All muscle activity occurs within the ascending limb of the LT curve, meaning the muscle only becomes stronger as it is elongated to its maximum length. For a given walking profile (which determines the muscle length profile), every muscle is capable of generating 70% of its maximum tension at its

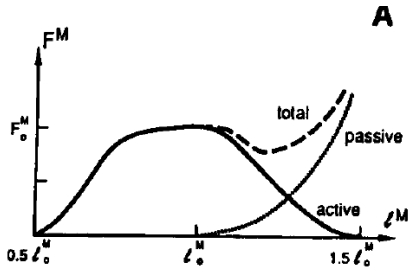

Fig. 4: Nominal length-tension curve for muscle

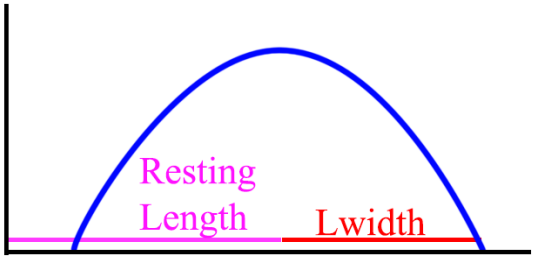

Fig. 5: Simplified LT curve in Animatlab

minimum length and 100% of its maximum tension at its maximum length. Based on these assumptions and Animatlab's LT formula, L_{width} can be calculated for each muscle:

$$
\begin{aligned}
T(L) &= \big(1 - \frac{(L - L_{rest})^2}{L_{width}^2}\big) * 100 \\
.3 &= \frac{(L_{min} - L_{max})^2}{L_{width}^2} \\
L_{width} &= \frac{|L_{min} - L_{max}|}{\sqrt{.3}} \\
L_{width} &= \frac{|L_{min} - L_{max}|}{\sqrt{.3}}
\end{aligned}
$$

$$
\begin{aligned}
U &= \sum_{i=1}^{38} F_i \\
U &= \sum_{i=1}^{38} F_i^2 \\
U &= \sum_{i=1}^{38} \frac{F_i}{F_{max,i}} \\
U &= \sum_{i=1}^{38} \big(\frac{F_i}{F_{max,i}}\big)^2 \\
U &= \sum_{i=1}^{38} F_i \Delta L_i
\end{aligned}
$$

Stimulus-Tension Curve The stimulus tension (ST) curve relates the membrane voltage of the motor neuron to the muscle tension. Other parameters from the ST equation include the maximum force amplitude, the steepness of the sigmoid, the x offset (in V), and the y-offset (in N). We are able to find the parameters for the ST curve under two assumptions. First, under the operating voltage of [-.01,-.1] mV, the contractile tension grows from 0% to 99% of the maximum tension. Second, that the ST curve should be centered at -50 mV. Based on these assumptions, the steepness and y-offset of the curve can

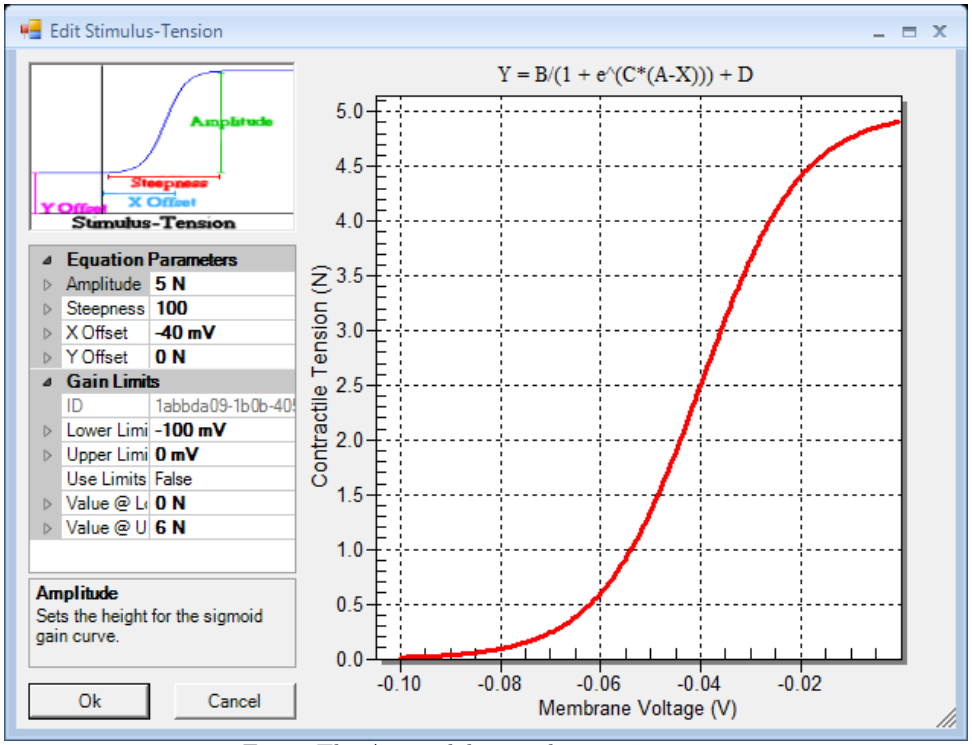

Fig. 6: The Animatlab stimulus-tension curve

be determined:

$$
\begin{aligned}
T(V) &= \frac{Amplitude}{1+e^{(x_{offset}-V)*steepness}} + y_{offset} \\
&= \frac{F_{max}}{1+e^{(x_{offset}-V)S}} + y_{offset} \\
T(-.01) = .99F_{max} &= \frac{F_{max}}{1+e^{-.04S}} + y_{offset} \\
T(-.1) = 0 &= \frac{F_{max}}{1+e^{.05S}} + y_{offset} \\
.99F_{max} &= \frac{F_{max}}{1+e^{-.04S}} - \frac{F_{max}}{1+e^{.05S}} \\
.99 &= \frac{1}{1+e^{-.04S}} - \frac{1}{1+e^{.05S}} \\
S &= 121.465
\end{aligned}
$$

$$
\begin{aligned}
.99F_{max} &= \frac{F_{max}}{1+e^{-.04S}} + y_{offset} \\
.99F_{max} &= \frac{F_{max}}{1+e^{-4.858}} + y_{offset} \\
y_{offset} &= F_{max}\left(.99 - \frac{1}{1+e^{-4.858}}\right) \\
y_{offset} &= -.002294F_{max}
\end{aligned}
$$

Muscle Moment Arms As a natural progression of analyzing the biomechanics of the model, the development of moment arm profiles during gait was developed. A moment arm calculation process developed from fundamental principles is a useful tool for analyzing the force generating capabilities of specific muscles in the model. This work led to a publication in the Journal of Biomimetics[10].

Muscle moment arms are developed by projecting muscle paths onto a plane on interest and then measuring the shortest distance from the joint center to the free muscle segment. In the case of 2D walking, the plane of interest is the sagittal plane. Since muscles often contain multiple via points and

those via points are often stationary relative to one another, the moment arm was calculated based on the segment of muscle that actively undergoes contraction during walking.

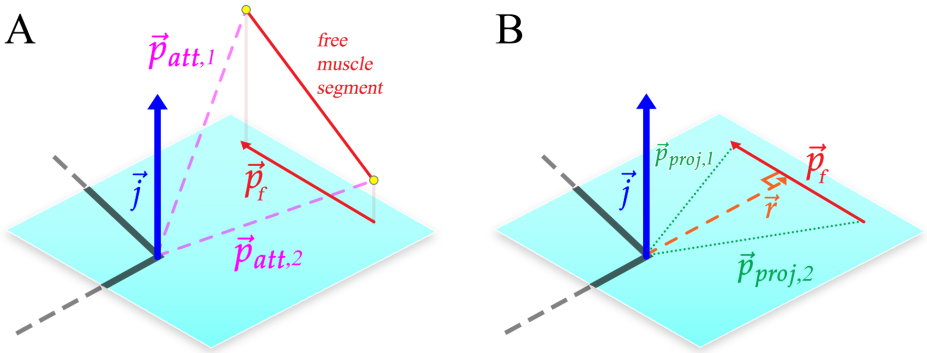

Fig. 7: The moment arm calculation example

3.2 Aim 2 - Calculate motorneuron activation profiles for complete hindlimb actuation

The simplest method of developing motorneuron signals is to first calculate joint torque about each joint and then decompose the total torque profile into individual muscle forces. This decomposition process has an infinite solution set, as individual muscle contributions can be combined in infinite permutations to generate the torque profile. First, an accurate total torque profile was established based on data from project collaborators. Next, the biomechanics of the system were considered to determine the impact of passive and active torque on the system. Finally, the complete torque profile was decomposed into individual muscle forces through a linear optimization technique.

The overall torque profile was calculated for both the stance and swing phase of walking. Stance phase mean joint torque was calculated for rat hindlimb joints during graded walking[11]. A Simulink model of the hind limb was was developed to determine joint torque during swing phase.

To determine torque generating muscle contributions, the passive torque due to body weight must be removed from the overall signal. Using ground reaction forces, it is possible to treat the leg like a multi-segmented arm with a force at the end effector. Joint torques can be calculated by constructing a spatial manipulator Jacobian[12], which combines the joint axes and positions. The composition of the spatial manipulator Jacobian is a 6×n matrix of the form:

$$\mathbf{J}^s_{st} = \begin{bmatrix} -\overrightarrow{\omega_n} \times \overrightarrow{q_n} \\ \overrightarrow{\omega_n} \end{bmatrix}.$$

where ω represents the joint axis and q_n represents a joint's global coordinates. Load torques are calculated using ground reaction force data[13] from the literature. With the spatial manipulator Jacobian and the ground reaction forces, the sagittal plane load torque in all three joints can be calculated using,

$$\overrightarrow{\tau} = (\mathbf{J}^s_{st})^T \overrightarrow{F_s}.$$

Active joint torque is the summation of individual muscle torques about each joint. With a method for calculating muscle moment arms in place, the only thing left is to calculate the muscle forces to generate the total torque profile. However, this is an infinite solution space making the outright distribution of muscle forces difficult. To address this problem a linear optimization has been applied.

Linear optimization is appropriate for this problem since it involves the summation of torques. The only difficulty remaining is determining the ideal cost function. The linear optimization process follows the form

$$min\ f^T x\ such\ that \begin{cases} \mathbf{A_{eq}} \cdot \overrightarrow{x} = \overrightarrow{b_{eq}} \\ \overrightarrow{lb} \leq \overrightarrow{x} \leq \overrightarrow{ub} \end{cases}$$

For this application, the muscle forces are represented by the vector $\overrightarrow{x}$, the muscle moment arms are compiled in $\mathbf{A_{eq}}$, and the torques are stored in $\overrightarrow{b_{eq}}$.

$$\begin{bmatrix} \sum_{i=1}^{38} p_{1,i} F_i \\ \sum_{i=1}^{38} p_{2,i} F_i \\ \sum_{i=1}^{38} p_{3,i} F_i \end{bmatrix} = \begin{bmatrix} \tau_1 \\ \tau_2 \\ \tau_3 \end{bmatrix}$$

Where we're seeking to minimize some function, for example the sum of the muscle forces:

$$min \sum_{i=1}^{38} F_i$$

The results of this minimization are promising and demonstrate a rudimentary capability of distributing muscle forces to accommodate the torque profile. However, this method results in force profiles with a number of biologically unrealistic results. First, oftentimes muscle becomes saturated at the maximum for for extended periods of time, seeming to "plateau" while moving the joint. Second, complementary muscles tend to switch on and off rapidly, rather than a smooth, gradual hand off of responsibility. Third, not all muscles are represented in the force profile. Although it's to be expected that not every single muscle is activated throughout walking, one would expect that all muscles would contribute *something* to locomotion at some point.

Now that a force profile has been developed, the question becomes how to translate that into motorneuron activation signals. In the past, this was done by using the Hill equation to solve for the necessary activation. Once this motorneuron signal is determined, though, it will need to be implemented in Animatlab. As this system has grown from six hindlimb muscles to thirty-eight, the demands of this neural system design increases as well. In order to address the demands of neural design, it became necessary to develop a tool for large-scale synthetic nervous system design.

A Neural Subsystem Design Tool This work was presented at ShowCASE 2019 in the form of a poster presentation. A Matlab GUI application has been developed for the design of large-scale synthetic nervous systems (SNSs). This work involves a user-interactive front end similar to Animatlab in which users are able to place, drag/drop, and delete neurons in a work environment. They are able to add different synaptic connections between the neurons and input parameter values for each node individually.

This system simultaneously records the node information (neurons and synapses) during subnetwork creation. Once a subnetwork has been defined, the user is able to export it or generate an Animatlab project file for simulation. This allows users to create networks that are useful for them (a CPG unit, for example) and rapidly deploy them in different SNSs they are working on.

An additional benefit of this software is the ability to immediately generate functional subunits[14] by selecting multiple neurons.

References

1. A. Hunt, N. Szczecinski, and R. Quinn, "Development and Training of a Neural Controller for Hind Leg Walking in a Dog Robot," *Frontiers in Neurorobotics*, vol. 11, 2017.
2. A. Hunt, M. Schmidt, M. Fischer, and R. D. Quinn, "Neuromechanical Simulation of an Inter-leg Controller for Tetrapod Coordination," in *Biomimetic and Biohybrid Systems* (A. Duff, N. F. Lepora, A. Mura, T. J. Prescott, and P. F. M. J. Verschure, eds.), Lecture Notes in Computer Science, pp. 142–153, Springer International Publishing, 2014.
3. A. J. Hunt, N. S. Szczecinski, E. Andrada, M. Fischer, and R. D. Quinn, "Using Animal Data and Neural Dynamics to Reverse Engineer a Neuromechanical Rat Model," in *Biomimetic and Biohybrid Systems* (S. P. Wilson, P. F. Verschure, A. Mura, and T. J. Prescott, eds.), Lecture Notes in Computer Science, pp. 211–222, Springer International Publishing, 2015.
4. W. L. Johnson, D. L. Jindrich, R. R. Roy, and V. Reggie Edgerton, "A three-dimensional model of the rat hindlimb: Musculoskeletal geometry and muscle moment arms," *Journal of Biomechanics*, vol. 41, pp. 610–619, Jan. 2008.
5. F. Young, A. J. Hunt, and R. D. Quinn, "A Neuromechanical Rat Model with a Complete Set of Hind Limb Muscles," in *Biomimetic and Biohybrid Systems*, (Paris, France), pp. 527–537, Springer, July 2018.
6. E. C. Greene, *Anatomy of the rat.* New York: Hafner Publishing Co., 1955.

7. W. L. Johnson, D. L. Jindrich, H. Zhong, R. R. Roy, and V. R. Edgerton, "Application of a Rat Hindlimb Model: A Prediction of Force Spaces Reachable Through Stimulation of Nerve Fascicles," *IEEE Transactions on Biomedical Engineering*, vol. 58, pp. 3328–3338, Dec. 2011.
8. C. M. Eng, L. H. Smallwood, M. P. Rainiero, M. Lahey, S. R. Ward, and R. L. Lieber, "Scaling of muscle architecture and fiber types in the rat hindlimb," *Journal of Experimental Biology*, vol. 211, pp. 2336–2345, July 2008.
9. F. E. Zajac, "Muscle and tendon: properties, models, scaling, and application to biomechanics and motor control.," *Critical reviews in biomedical engineering*, vol. 17, no. 4, pp. 359–411, 1989.
10. F. Young, C. Rode, A. Hunt, and R. Quinn, "Analyzing Moment Arm Profiles in a Full-Muscle Rat Hindlimb Model," *Biomimetics*, vol. 4, p. 10, Mar. 2019.
11. E. Andrada, J. Mämpel, A. Schmidt, M. Fischer, A. Karguth, and H. Witte, "From biomechanics of rats' inclined locomotion to a climbing robot," *International Journal of Design & Nature and Ecodynamics*, vol. 8, pp. 192–212, Sept. 2013.
12. R. M. Murray, Z. Li, and S. S. Sastry, *A Mathematical Introduction to Robotic Manipulation.* CRC Press, 1994.
13. G. D. Muir and I. Q. Whishaw, "Ground reaction forces in locomoting hemi-parkinsonian rats: a definitive test for impairments and compensations," *Experimental Brain Research*, vol. 126, pp. 307–314, May 1999.
14. N. S. Szczecinski, A. J. Hunt, and R. D. Quinn, "A Functional Subnetwork Approach to Designing Synthetic Nervous Systems That Control Legged Robot Locomotion," *Frontiers in Neurorobotics*, vol. 11, 2017.